Available online at www.sciencedirect.com
SCIENCE DIRECT®
Chemical Physics Letters 423 (2006) 76–80
CHEMICAL PHYSICS LETTERS
www.elsevier.com/locate/cplett

Quantum bath effects on nonadiabatic reaction rates

Hyojoon Kim *, Raymond Kapral

Chemical Physics Theory Group, Department of Chemistry, University of Toronto, Toronto, Ont., Canada M5S 3H6

Received 4 November 2005; in final form 8 March 2006
Available online 16 March 2006

Abstract

Quantum chemical reactions, where the reaction coordinate is coupled to a bath or environment comprising other degrees of freedom of the system, are investigated. We approximate the quantum time evolution by quantum–classical Liouville surface-hopping dynamics. Within this framework, we explore the effect on the reaction rate of sampling the reaction coordinate and bath initial conditions from quantum and classical distributions. We find that the rate constant determined from quantum bath sampling is lower than that obtained from classical bath sampling. This is also shown to be the case for a simple analytically solvable two-dimensional reaction model.

1. Introduction

Quantum rate processes occurring in condensed phase or other complex systems are influenced by coupling to the environment in which the reactions take place. Such coupling can lead to nonadiabatic effects where various excited state surfaces participate in the reaction dynamics. Reaction rate constants may be expressed in terms of reactive-flux correlation expressions whose computation entails carrying out quantum evolution of operators and sampling from quantum equilibrium distributions [1]. Since the simulation of fully quantum dynamics for systems with a large number of degrees of freedom is difficult, quantum–classical dynamical schemes have been constructed to describe the evolution in systems where quantum dynamics of a subset of degrees of freedom is coupled to classical evolution of the environment [2,3]. We consider quantum–classical Liouville dynamics [4–7] which is accurate in many circumstances; for example, it is exact for a quantum system bilinearly coupled to a harmonic bath. In this quantum–classical Liouville context, we consider the effects on the reaction rate of also approximating the equilibrium structure of the environment by classical mechanics.

The effects of quantum and classical treatments of the bath on vibrational relaxation have been studied earlier [8,9] where it was shown that care had to be exercised when mixing quantum and classical levels of description of the vibrational and bath dynamics and structure. Quantum bath equilibrium structure is also incorporated in many studies of quantum reaction rates, especially for harmonic bath models [10–14].

For the case where the reaction coordinate depends on environmental variables, we contrast the quantum and classical treatments of the reaction coordinate with similar treatments of the bath variables. We also investigate a simple analytically solvable two-variable system whose solution provides additional insight into the effects of quantum and classical bath sampling on the reaction rate. The main results of these computations are that, compared to a classical description, a quantum treatment of the equilibrium structure of the reaction coordinate increases the reaction rate constant while a quantum treatment of the bath lowers the rate constant.

2. Quantum rate and system specification

The systems in which we are interested may be usefully partitioned into a quantum subsystem $\mathscr{S}$ and a quantum environment $\mathscr{E}$. The Hamiltonian for the system can be written as $\hat{H} = \hat{P}^2/2M + \hat{h}(R)$, the sum of the kinetic

* Corresponding author. Fax: +1 416 978 5325.
E-mail addresses: hkim@chem.utoronto.ca (H. Kim), rkapral@chem.utoronto.ca (R. Kapral).

0009-2614/$ - see front matter © 2006 Elsevier B.V. All rights reserved.
doi:10.1016/j.cplett.2006.03.025

energy of the bath particles and the Hamiltonian for the quantum subsystem in the field of the fixed bath particles, respectively. The adiabatic states are the eigenfunctions of the eigenvalue problem, $\hat{h}(R)\,|\alpha;R\rangle = E_\alpha(R)\,|\alpha;R\rangle$ and $E_\alpha(R)$ are the corresponding adiabatic energies. In such a system, consider a chemical reaction $\mathrm{A} \rightleftharpoons \mathrm{B}$ between metastable A and B species. Suppose these species are characterized by operators $\hat{N}_\mathrm{A}$ and $\hat{N}_\mathrm{B}$, respectively. The time dependent rate coefficient for this reaction, whose plateau value gives the rate constant, was derived earlier [15,16] and can be written as

$$k_{\mathrm{AB}}(t) = \frac{1}{n_\mathrm{A}^{\mathrm{eq}}} \sum_\alpha \sum_{\alpha' \geqslant \alpha} (2 - \delta_{\alpha'\alpha}) \times \int \mathrm{d}X\, \mathrm{Re}\left[N_\mathrm{B}^{\alpha\alpha'}(X,t) W_\mathrm{A}^{\alpha'\alpha}\left(X, \frac{\mathrm{i}\hbar\beta}{2}\right)\right]. \quad (1)$$

Here $X = (R, P)$ denotes the set of phase space variables of $\mathscr{E}$ in the Wigner representation and $W_\mathrm{A}^{\alpha'\alpha}$ is the spectral density function that contains all information on the quantum equilibrium structure of the entire system. The time evolution of the species variable $N_\mathrm{B}^{\alpha\alpha'}(X,t)$ is given by quantum–classical Liouville dynamics [6].

We consider the evaluation of this rate expression for a model reactive system that captures many of the generic features of quantum reactions in the condensed phase. The quantum subsystem $\mathscr{S}$ is a two-level system with Hamiltonian $\hat{H}_s$. This two-level system is coupled directly to a quartic oscillator with Hamiltonian $\hat{H}_n$ which is, in turn, coupled to a bath ($\mathscr{B}$) of harmonic oscillators with Hamiltonian $\hat{H}_\mathrm{b}$. The quartic oscillator and bath constitute the environment $\mathscr{E}$ of the two-level quantum subsystem. The Hamiltonian operator in the diabatic basis of the two-level system can be written as [17]

$$\mathbf{H} = \begin{pmatrix} V_n(R_0) + \hbar\gamma(R_0) & -\hbar\Omega \\ -\hbar\Omega & V_n(R_0) - \hbar\gamma(R_0) \end{pmatrix} + \left(\frac{P_0^2}{2M_0} + \sum_{j=1}^{v-1} \frac{P_j^2}{2M_j} + V_{\mathrm{b}(n)}(R_\mathrm{b}; R_0)\right)\mathbf{I}. \quad (2)$$

Here, the quartic potential $V_n(R_0) = -M_0\omega_0^2 R_0^2/2 + AR_0^4/4$ and the harmonic bath potential, including coupling to the quartic oscillator, is $V_{\mathrm{b}(n)}(R_\mathrm{b}; R_0) = \frac{1}{2}\sum_{j=1}^{v-1} M_j\omega_j^2 \left(R_j - c_j\omega_j^{-2}M_j^{-1}R_0\right)^2$, where M_j and ω_j are the mass and frequency for the jth oscillator. We choose $\gamma(R_0) = \gamma_0 R_0$ with the parameter γ_0 specifying the strength of the bilinear coupling between the two-level system and the quartic oscillator. Half the energy gap is denoted by $\hbar\Omega$. The total number of degrees of freedom is v. Including the coupling terms, the Hamiltonian may be written as $\hat{H} = \hat{H}_{sn} + \hat{H}_{\mathrm{b}(n)}$, where $\hat{H}_{sn}$ is the Hamiltonian for the coupled two-level system and quartic oscillator and $\hat{H}_{\mathrm{b}(n)}$ is the bath Hamiltonian including coupling to the quartic oscillator.

The adiabatic states $|\alpha;R_0\rangle$ and the corresponding adiabatic energies $E_\alpha(R)$ ($\alpha = 1, 2$) are obtained by diagonalizing this Hamiltonian [16]. The adiabatic energies are not symmetric in R_0 because of coupling of R_0 to the bath. Asymmetries arising from $V_n(R_0)$ or the coupling of R_0 to the quantum subsystem are easily treated using the quantum–classical formalism [18].

3. Quantum bath effects

To compute the reaction rate we choose the species operators to be $\hat{N}_\mathrm{A} = \theta(-R_0)$ and $\hat{N}_\mathrm{B} = \theta(R_0)$, where θ is the Heaviside step function, and take the dividing surface that separates the domains that contain the A and B metastable states to lie at $R_0^\ddagger = 0$. Then, assuming $\exp(-\beta\hat{H}) \approx \exp(\beta\hat{H}_{sn})\exp(-\beta\hat{H}_{\mathrm{b}(n)})$, singling out the barrier region and separating V_n into harmonic and remainder terms, we have shown that Eq. (1) can be written more explicitly as [16]

$$k_{\mathrm{AB}}(t) = \frac{1}{n_\mathrm{A}^{\mathrm{eq}}} \sum_\alpha \int \mathrm{d}X N_\mathrm{B}^{\alpha\alpha}(X,t)\rho_{sn}^{\alpha\alpha}(X_0)\rho_\mathrm{b}(X_\mathrm{b}; R_0), \quad (3)$$

where

$$\rho_{sn}^{\alpha\alpha}(X_0) = \frac{1}{Z_{sn}} \frac{\omega_0}{2\pi \sin 2u_0} \sqrt{\frac{2M_0u_0'}{\pi\beta\hbar^2}} \frac{\beta P_0}{M_0u_0'} \times \exp\left\{ -\beta\left(AR_0^4/4 \mp \sqrt{\Omega^2 + \gamma_0^2 R_0^2}\right) - \frac{2M_0u_0'}{\beta\hbar^2}R_0^2 - \frac{\beta}{2M_0u_0'}P_0^2\right\}, \quad (4)$$

and

$$\rho_\mathrm{b}(X_\mathrm{b}; R_0) = \frac{1}{Z_\mathrm{b}} \prod_j \frac{\beta\omega_j}{2\pi u_j''} \mathrm{e}^{-\frac{\beta}{u_j''}\left(\frac{1}{2M_j}P_j^2 + V_{\mathrm{b}(n)}(R_j;R_0)\right)}, \quad (5)$$

with $u_i' \equiv u_i \cot u_i$, $u_i'' = u_i \coth u_i$, and $u_i = \beta\hbar\omega_i/2$ and the sign is minus for the ground state ($\alpha = 1$) and plus for the excited state ($\alpha = 2$). In this approximation, the partition function may be factorized as $Z_\mathrm{Q} = Z_{sn}Z_\mathrm{b}$. There are also off-diagonal contributions to the rate. These off-diagonal terms scale as the product of the nonadiabatic coupling matrix element and the de Broglie wavelength of the reaction coordinate. These terms are negligible for our parameter values but may be nonnegligible for stronger nonadiabatic coupling [19].

The classical limits of the quantum equilibrium structure can be obtained by taking the high temperature limits of these expressions. Using the relations $\lim_{\beta\to 0}\sqrt{a/(\pi\beta)}\,\mathrm{e}^{-(a/\beta)R_0^2} = \delta(R_0)$ and $\lim_{\beta\to 0}u_0' = \lim_{\beta\to 0}u_j'' = 1$, we can easily obtain classical-limit expressions as

$$\rho_{sn}^{\alpha\alpha,\mathrm{cl}}(X_0) = \frac{1}{Z_{sn}^{\mathrm{cl}}} \frac{1}{2\pi\hbar}\delta(R_0)\frac{P_0}{M_0}\mathrm{e}^{-\frac{\beta}{2M_0}P_0^2 \pm \beta\Omega}, \quad (6)$$

and

$$\rho_\mathrm{b}^{\mathrm{cl}}(X_\mathrm{b}; 0) = \frac{1}{Z_\mathrm{b}^{\mathrm{cl}}} \prod_j \frac{\beta\omega_j}{2\pi} \mathrm{e}^{-\beta\left(\frac{1}{2M_j}P_j^2 + \frac{1}{2}M_j\omega_j^2R_j^2\right)}, \quad (7)$$

which agree with the results obtained earlier [17].

Eq. (3), along with the expressions in Eqs. (4)–(7), forms the basis of the calculations carried out in this Letter. We

label the results from quantum and classical treatments of the reaction coordinate as QR and CR, respectively. Similarly, we use the labels of QB and CB for quantum and classical treatments of the bath.

The numerical results were obtained using an Ohmic spectral density as $J(\omega) = \pi \sum c_j^2/(2M_j\omega_j)\delta(\omega - \omega_j)$, where $c_j = (\xi\hbar\Delta\omega M_j)^{1/2}\omega_j$, $\omega_j = -\omega_c \ln(1 - j\Delta\omega/\omega_c)$ and $\Delta\omega = \frac{\omega_c}{\nu-1}\left(1 - e^{-\omega_{max}/\omega_c}\right)$ with ω_c the cutoff frequency [20]. Dimensionless units are used with coordinates scaled by $\sqrt{M\omega_c/\hbar}$ and momenta by $\sqrt{\hbar M\omega_c}$ [17]. In these units the mass dependence enters through the scaled coupling constants as $c_j \leftarrow c_j/(M_j\omega_j^2)\sqrt{M_j/M_0}$ or, equivalently, the Kondo parameter ξ. The number of bath harmonic oscillators is $N_b = 100$ so that $\nu = 101$. We have chosen $A = 0.05$ and $\omega_0 = 1$ so that the bare barrier height is 5 in dimensionless units. The coupling constants are $\Omega = 0.1$ and $\gamma_0 = 0.1$. For these parameters, the ground and excited potential surfaces are similar to each other and the reactant partition function can be approximated as $(n_A^{eq} Z_Q)^{-1} \approx e^{\beta V_r} \sinh u_r \prod_j 2\sinh u_j$ with ω_r the well frequency and V_r the bare potential at the bottom of the well. The transmission coefficient is defined as $\kappa_{AB}(t) = k_{AB}(t)/k_{AB}^{TST}$, where the transition state value is given by $k_{AB}^{TST} \approx (4\pi)^{-1}\omega_r e^{\beta V_r}(e^{-\beta\hbar\Omega} + e^{\beta\hbar\Omega})$.

We refer to Refs. [21,22] for the details of the nonadiabatic quantum–classical evolution. Only the sampling of initial conditions differs from that in earlier studies of quantum–classical reaction rates. The initial distribution of X is sampled from distributions proportional to Eqs. (4) and (5) or Eqs. (6) and (7).

In Fig. 1, we plot the transmission coefficients κ_{AB}^{QRQB}, κ_{AB}^{QRCB}, κ_{AB}^{CRCB}, and κ_{AB}^{CRQB}, for various values of Kondo parameter ξ. The change in the rate constant arising from quantum and classical treatments of the reaction coordinate is much greater than the corresponding change for quantum and classical treatments of the bath equilibrium structure. The incorporation of quantum effects on the reaction coordinate is known to increase the rate due to quantum tunneling and our results confirm such an increase in the rate. Quantum bath effects, on the other hand, decrease the rate by roughly 5–10% for our model system. This is consistent with earlier numerical studies [23], where a small difference was found between the results obtained by quantizing the entire system and quantizing only the subsystem. Therefore, κ_{AB}^{QRCB} for a quantum treatment of the reaction coordinate and a classical treatment of the bath gives the largest rate and κ_{AB}^{CRQB} gives the smallest rate. All approximations to the rate show similar turnover behavior for small ξ.

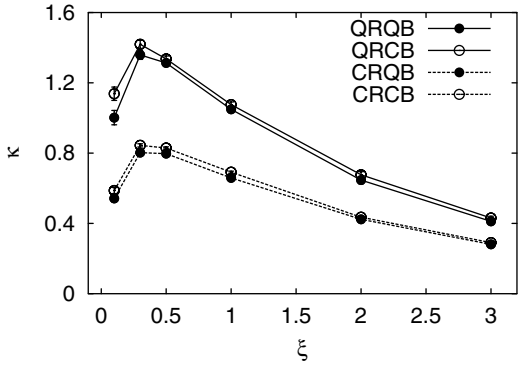

Fig. 1. Transmission coefficient vs. ξ for $\beta = 2$. The solid and dashed lines denote quantum (QR) and classical (CR) treatments of the reaction coordinate, respectively, while filled and open circles denote quantum (QB) and classical (CB) treatments of the bath, respectively.

Comparing Eq. (5) with Eq. (7), we can relate these two expressions by the following convolution equation [24]:

$$\rho_b(X_b) = \int dX_b' \, g(X_b' - X_b)\rho_b^{cl}(X_b'), \tag{8}$$

where

$$g(X_b) = \frac{Z_b^{cl}}{Z_b}\prod_j \frac{\beta\omega_j}{2\pi(u_j'' - 1)} e^{-\frac{\beta}{u_j''-1}\left(\frac{1}{2M_j}P_j^2 + \frac{1}{2}M_j\omega_j^2 R_j^2\right)}. \tag{9}$$

so that the classical distribution is broadened by the quantum dispersion function g to yield the quantum distribution. We define the average value of $N_B^{\alpha\alpha}(X,t)$ over the quantum dispersion of the bath as $\langle N_B^{\alpha\alpha}(X',t)\rangle_b^g(X,t) = \int dX_b' g(X_b' - X_b) N_B^{\alpha\alpha}(X',t)$, where the Gaussian function $g(X_b' - X_b)$ is centered at the phase point X_b sampled from the classical bath distribution. Then, with help of Eq. (8), the reaction rate equation (3) for the quantum bath sampling can also be written as

$$k_{AB}^{QB}(t) = \frac{1}{n_A^{eq}}\sum_\alpha \int dX \langle N_B^{\alpha\alpha}(X',t)\rangle_b^g(X,t)\rho_{sn}^{\alpha\alpha}(X_0)\rho_b^{cl}(X_b;R_0). \tag{10}$$

This equation has the same form as that for classical bath sampling, which is

$$k_{AB}^{CB}(t) = \frac{1}{n_A^{eq}}\sum_\alpha \int dX N_B^{\alpha\alpha}(X,t)\rho_{sn}^{\alpha\alpha}(X_0)\rho_b^{cl}(X_b;R_0), \tag{11}$$

except that $N_B^{\alpha\alpha}(X,t)$ is replaced by its average over the quantum dispersion.

Our numerical results show that $k_{AB}^{QB}(t) \leqslant k_{AB}^{CB}(t)$ so that the additional average over the quantum dispersion of the bath position and momentum variables leads to more rapid decay of the species variable and a reduction of the rate.

For the model parameters used in this study, quantum bath effects tend to be larger for smaller values of ξ corresponding to weaker coupling to the bath modes. This trend is also consistent with the fact that coupling between the reaction coordinate and the bath results in a reduction in the quantum character of the reaction coordinate [25,26]. This effect becomes more pronounced for stronger coupling. The emergence of a quantum–classical description was shown to be a consequence of decoherence arising from coupling to bath degrees of freedom [27].

In Fig. 2, we show how the various approximations to the rate constant depend on β for a small value of the Kondo parameter, $\xi = 0.1$, for which quantum bath effects are discernible in the data. The differences between the

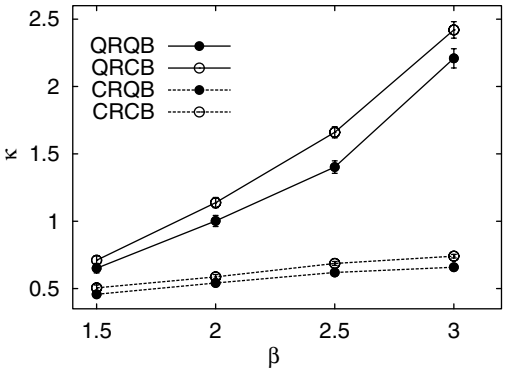

Fig. 2. Transmission coefficient vs. β for $\xi = 0.1$. The symbols are the same as in Fig. 1.

various approximations to the transmission coefficients increase as the temperature decreases. The rate constant results obtained using a quantum treatment of the reaction coordinate increase strongly with β. This is expected since quantum effects will play a larger role at low temperatures. Indeed, quantum bath effects which reduce the rate also become significant at low temperatures.

4. Two-dimensional system

In the study in the previous section, the differences arising from quantum and classical treatments of the bath and reaction coordinate equilibrium structure were deduced from an analysis of the numerical data. Here we consider a very simple reaction model where these effects can be studied analytically.

The model consists of a reaction coordinate R_0 governed by harmonic potentials in the barrier and well regions,

$$V_n(R_0) \approx V_0 - \frac{1}{2}M_0\omega_0^2 R_0^2 \text{ (barrier)} \tag{12}$$

$$\approx \frac{1}{2}M_0\omega_r^2 R_0^2 \text{ (well)} \tag{13}$$

coupled to a single bath oscillator. This is a simplified version of a model investigated in detail previously [10,11,28,29]. Absorbing boundaries are imposed outside the barrier region to give a well-defined reaction rate. We can write the Hamiltonian in separable form as two independent harmonic oscillators by making a normal mode transformation [11,28,29]. We can diagonalize the force constant matrix to obtain the eigenvalues or renormalized frequencies $\tilde{\omega}_0^2$ and $\tilde{\omega}_1^2$ as

$$\tilde{\omega}_{0,1}^2 = \pm\frac{1}{2}\left(\omega_0^2 - \frac{c_1^2}{\omega_1^2 M_0 M_1} - \omega_1^2\right) + \frac{1}{2} \times \sqrt{\left(\omega_1^2 + \omega_0^2 - \frac{c_1^2}{\omega_1^2 M_0 M_1}\right)^2 + \frac{4c_1^2}{M_0 M_1}}, \tag{14}$$

where c_1 is the coupling constant in Section 3. We are interested in the unstable mode, so we assume $\omega_0^2 > c_1^2/(\omega_1^2 M_0 M_1)$ to make $\tilde{\omega}_0^2$ positive. Since $c_1^2 \geqslant 0$, we obtain the inequality $\omega_0^2 - c_1^2/(\omega_1^2 M_0 M_1) \leqslant \tilde{\omega}_0^2 \leqslant \omega_0^2$, where the equal sign corresponds to the case $c_1 = 0$. The renormalized phase space variables $\widetilde{X}$ are obtained by a linear transformation matrix L as $\widetilde{R}_j = \sum_i L_{ji} M_i^{1/2} R_i$ and $\widetilde{P}_j = \sum_i L_{ji} M_i^{-1/2} P_i$. The transformation matrix is given by [30]

$$L = \begin{pmatrix} \cos\phi & -\sin\phi \\ \sin\phi & \cos\phi \end{pmatrix}, \tag{15}$$

with $\cos^2\phi = (\omega_1^2 + \tilde{\omega}_0^2)/(-\omega_0^2 + c_1^2/(\omega_1^2 M_0 M_1) + \omega_1^2 + 2\tilde{\omega}_0^2)$.

In terms of renormalized phase space coordinates, the time dependent rate takes the form,

$$k_{AB}(t) = \frac{1}{n_A^{eq}} \int d\widetilde{X}\,\theta\{R_0(t)\} W_A\left(\widetilde{X}, \frac{i\hbar\beta}{2}\right), \tag{16}$$

where, by direct calculation, the spectral density function is found to be

$$W_A\left(\widetilde{X}, \frac{i\hbar\beta}{2}\right)\widetilde{Z}_0 e^{\beta V_0} = \left(\frac{1}{2\pi\hbar}\right)^2 \frac{1}{\cos\tilde{u}_0 \cosh\tilde{u}_1 \hbar} \times \sqrt{\frac{2\tilde{u}_0'\tilde{u}_1''}{\pi\beta C}}\left(\frac{\cos\phi}{\cos\tilde{u}_0}\widetilde{P}_0 + \frac{\sin\phi}{\cosh\tilde{u}_1}\widetilde{P}_1\right) \times e^{-\frac{\beta}{2\tilde{u}_0'}\widetilde{P}_0^2 - \frac{\beta}{2\tilde{u}_1''}\widetilde{P}_1^2} \times \exp\left[-\frac{2}{\beta\hbar^2 C} \times \left\{\left(C\tilde{u}_0' - \left(\frac{\sin\phi}{\sin\tilde{u}_0}\tilde{u}_0\right)^2\right)\widetilde{R}_0^2 + \left(C\tilde{u}_1'' - \left(\frac{\cos\phi}{\sin\tilde{u}_1}\tilde{u}_1\right)^2\right)\widetilde{R}_1^2 + \sin 2\phi \frac{\tilde{u}_0\tilde{u}_1}{\sin\tilde{u}_0 \sinh\tilde{u}_1}\widetilde{R}_0\widetilde{R}_1\right\}\right], \tag{17}$$

where $C = \tilde{u}_0' \sin^2\phi + \tilde{u}_1'' \cos^2\phi$ with $\tilde{u}_i = \beta\hbar\tilde{\omega}_i/2$ and $\widetilde{Z}_0$ is the partition function for the renormalized reaction coordinate. Since $\widetilde{R}_0(t) = \widetilde{R}_0 \cosh\tilde{\omega}_0 t + (\widetilde{P}_0/\tilde{\omega}_0)\sinh\tilde{\omega}_0 t$, the Heaviside function in the long time limit can be easily obtained as [31] $\theta\{R_0(\infty)\} = \theta(\widetilde{R}_0 + \widetilde{P}_0/\tilde{\omega}_0)$.

The rate constant can be calculated from Eq. (16) by inserting the expression for $W_A\left(\widetilde{X}, \frac{i\hbar\beta}{2}\right)$ given in Eq. (17) and preforming the integrals to obtain

$$k_{AB} = \frac{1}{n_A^{eq}\widetilde{Z}_0}\frac{\tilde{\omega}_0}{4\pi\sin\tilde{u}_0} e^{-\beta V_0}. \tag{18}$$

This exact result is the same as that for a system with a renormalized coordinate $\widetilde{X}_0$ and a single parabolic barrier with frequency $\tilde{\omega}_0$. Therefore, if we choose the reaction coordinate to be $\widetilde{R}_0$ instead of R_0 and use the expression for W_A for a simple parabolic system, we also obtain Eq. (18) even though W_A and the transient rate $k_{AB}(t)$ are different.

For this two-dimensional system, we can analyze the quantum bath effects by using the same approximations for the spectral density function discussed earlier for the two-level reaction model. The W_A function may be rearranged to give

$$W_A\left(X, \frac{i\hbar\beta}{2}\right)Z_0 e^{\beta V_0} = \frac{\omega_0}{2\pi\sin 2u_0}\rho_n(X_0)\rho_b(X_1; R_0), \tag{19}$$

and the quantum or classical equilibrium forms of ρ_n and ρ_b analogous to those in Eqs. (4)–(7) can be inserted to yield the results.

If we treat the reaction coordinate quantum mechanically, the following rate constants are obtained with the quantum or classical equilibrium structure of the bath

$$k_{AB}^{QRQB} = \frac{1}{n_A^{eq} Z_0} \frac{\tilde{\omega}_0}{4\pi \sin u_0} e^{-\beta V_0} \times \left(1 - \frac{(\omega_0^2 - \tilde{\omega}_0^2)(4\tilde{u}_0^2 + u_0'^2 - u_0' u_1'') \cos^2 u_0}{\omega_0^2 u_0'^2}\right)^{-\frac{1}{2}}, \quad (20)$$

$$k_{AB}^{QRCB} = \frac{1}{n_A^{eq} Z_0} \frac{\tilde{\omega}_0}{4\pi \sin u_0} e^{-\beta V_0} \times \left(1 - \frac{(\omega_0^2 - \tilde{\omega}_0^2)(4\tilde{u}_0^2 + u_0'^2 - u_0') \cos^2 u_0}{\omega_0^2 u_0'^2}\right)^{-\frac{1}{2}}. \quad (21)$$

Since $\omega_0^2 \geqslant \tilde{\omega}_0^2$ and $u_1'' > 1$, k_{AB}^{QRCB} is always larger than k_{AB}^{QRQB}, which implies that incorporation of quantum bath effects always reduce the reaction rate. (We restrict ourselves to the case of $u_0' > 0$.) We note that k_{AB}^{QRQB} and k_{AB} in Eq. (18) become identical in the small β limit and which of k_{AB}^{QRQB} and k_{AB} is larger depends on the sign of the term $4\tilde{u}_0^2 + u_0'^2 - u_0' u_1''$. The rate constant k_{AB}^{QRCB} is always larger than k_{AB}.

We plot the ratio $k_{AB}^{QRCB}/k_{AB}^{QRQB}$ as a function of c_1 for two values of temperature in Fig. 3. The ratio is larger for the lower temperature as expected. A maximum in the quantum bath effect is seen in the curve for $\beta = 2$. This arises from the fact that, in the small c_1 limit, the value of k_{AB}^{QRCB} is similar to that of k_{AB}^{QRQB} since very weak coupling between two oscillators hardly affects the dynamics. Quantum bath effects in the reaction coordinate come into play as the coupling increases but very strong coupling reduces the quantum character of the reaction coordinate in the large c_1 limit. Similar results can be observed in Fig. 1. For $\beta = 1$, there is no maximum since the quantum effects are less pronounced at high temperatures.

If we treat the reaction coordinate classically, the rate constants for quantum and classical treatments of the bath, respectively, are given by

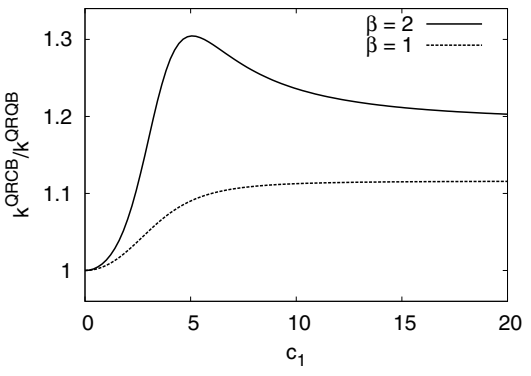

Fig. 3. Ratio of $k_{AB}^{QRCB}/k_{AB}^{QRQB}$ vs. c_1 for $\beta = 1$ and 2. Parameter values: $\omega_0 = 1$, $\omega_1 = 2$, and $M_0 = M_1 = 1$.

$$k_{AB}^{CRQB} = \frac{1}{n_A^{eq} Z_0^{cl}} \frac{\tilde{\omega}_0}{4\pi u_0} e^{-\beta V_0} \left(1 + \frac{(u_1'' - 1)(\omega_0^2 - \tilde{\omega}_0^2)}{\omega_0^2}\right)^{-\frac{1}{2}}, \quad (22)$$

$$k_{AB}^{CRCB} = \frac{1}{n_A^{eq} Z_0^{cl}} \frac{\tilde{\omega}_0}{4\pi u_0} e^{-\beta V_0}. \quad (23)$$

From these results one can easily confirm that the inequality, $k_{AB}^{CRCB} > k_{AB}^{CRQB}$, always holds. This inequality is the same as that inferred from the numerical data on the more complex reaction model where a two-level system was coupled directly to a reaction coordinate which was in turn coupled to a many-body harmonic oscillator bath. Consequently, our results provide some insight into how quantum and classical treatments of the bath equilibrium structure influence chemical reaction rates.

Acknowledgements

This work was supported in part by a grant from the Natural Sciences and Engineering Research Council of Canada. We thank P.J. Rossky for a useful discussion concerning Ref. [24].

References

[1] T. Yamamoto, J. Chem. Phys. 33 (1960) 281.
[2] M. Herman, Annu. Rev. Phys. Chem. 45 (1994) 83.
[3] J.C. Tully, in: D.L. Thompson (Ed.), Modern Methods for Multidimensional Dynamics Computations in Chemistry, World Scientific, New York, 1998, p. 34.
[4] I.V. Aleksandrov, Z. Naturforsch. 36 (1981) 902.
[5] V.I. Gerasimenko, Repts. Acad. Sci. Ukr. SSR. 10 (1981) 65.
[6] R. Kapral, G. Ciccotti, J. Chem. Phys. 110 (1999) 8919.
[7] R. Kapral, G. Ciccotti, in: P. Nielaba, M. Mareschal, G. Ciccotti (Eds.), In Bridging Time Scales: Molecular Simulations for the Next Decade, Springer-Verlag, Berlin, 2002, p. 445, and references therein.
[8] J.S. Bader, B.J. Berne, J. Chem. Phys. 100 (1994) 8359.
[9] S. Egorov, B.J. Berne, J. Chem. Phys. 107 (1997) 6050.
[10] P. Wolynes, Phys. Rev. Lett. 47 (1981) 968.
[11] E. Pollak, Chem. Phys. Lett. 127 (1986) 178.
[12] P. Hanggi, P. Talkner, M. Borkovec, Rev. Mod. Phys. 62 (1990) 251, and references therein.
[13] M. Topaler, N. Makri, J. Chem. Phys. 101 (1994) 7500.
[14] H. Wang, X. Sun, W. Miller, J. Chem. Phys. 108 (1998) 9726.
[15] H. Kim, R. Kapral, J. Chem. Phys. 122 (2005) 214105.
[16] H. Kim, R. Kapral, J. Chem. Phys. 123 (2005) 194108.
[17] A. Sergi, R. Kapral, J. Chem. Phys. 118 (2003) 8566.
[18] S. Nielsen, R. Kapral, G. Ciccotti, J. Stat. Phys. 101 (2000) 225.
[19] H. Kim, G. Hanna, R. Kapral (in preparation).
[20] N. Makri, J. Phys. Chem. B 103 (1999) 2823.
[21] D. MacKernan, R. Kapral, G. Ciccotti, J. Phys.: Condens. Matter 14 (2002) 9069.
[22] G. Hanna, R. Kapral, J. Chem. Phys. 122 (2005) 244505.
[23] T. Yamamoto, W.H. Miller, J. Chem. Phys. 122 (2005) 044106.
[24] H. Hwang, P.J. Rossky, J. Chem. Phys. 120 (2004) 11380.
[25] J. Poulsen, G. Nyman, P.J. Rossky, J. Chem. Phys. 119 (2003) 12179.
[26] J. Poulsen, G. Nyman, P.J. Rossky, J. Phys. Chem. A 108 (2004) 8743.
[27] K. Shiokawa, R. Kapral, J. Chem. Phys. 117 (2002) 7852.
[28] E. Pollak, J. Chem. Phys. 85 (1986) 865.
[29] I. Rips, E. Pollak, Phys. Rev. A 41 (1990) 5366.
[30] A. Dutra, J. Phys. A 25 (1992) 4189.
[31] E. Pollak, J. Liao, J. Chem. Phys. 108 (1998) 2733.